Neoplasia • Vol. 3, No. 1, 2001, pp. 80–87 80

www.nature.com/neo

Coregulation of Glucose Uptake and Vascular Endothelial Growth Factor (VEGF) in Two Small-Cell Lung Cancer (SCLC) Sublines *In Vivo* and *In Vitro*[1]

Minna W. B. Pedersen, Søren Holm, Eva L. Lund, Liselotte Højgaard and Paul E. G. Kristjansen

Laboratory of Experimental Oncology, Molecular Pathology, University of Copenhagen, PET and Cyclotron Unit, National University Hospital, Copenhagen, Denmark

Abstract

We examined the relationship between ^{18}F- labeled 2-fluro-2-deoxy-D-glucose (FDG) uptake, and expression of glucose transporters (GLUTs) in two human small-cell lung cancer (SCLC) lines CPH 54A and CPH 54B. Changes in the expression of GLUTs and vascular endothelial growth factor (VEGF) during 12-, 18-, and 24 hours of severe hypoxia *in vivo* (xenografts) and *in vitro* (cell cultures) were recorded for both tumor lines. The two SCLC lines are subpopulations of the same patient tumor. In spite of their common genomic origin they represent consistently different metabolic and microenvironmental phenotypes as well as treatment sensitivities. There were higher levels of Glut-1 protein in 54B and a correspondingly higher FDG uptake in this tumor line (P<.001). During hypoxia a significant upregulation of in VEGF mRNA, GLUT-1 mRNA, and Glut-1 and -3 protein occurred with a distinctly different time course in the two cell lines. A similar co-upregulation of GLUT and VEGF was seen in hypoxic tumors of both lines. There were no significant changes of HIF-1α mRNA during hypoxia in either of the cell lines. A more detailed understanding of such correlations between glucose metabolism, angiogenesis, and microenvironmental phenotype of tumors, by positron emission tomography (PET) and molecular techniques might further sophisticate our interpretation of glycolytic predominance in tumors as seen by ^{18}FFDG PET. *Neoplasia* (2001) **3,** 80–87.

Keywords: VEGF, GLUT-1, hypoxia, HIF-1α, small-cell lung cancer.

Introduction

The two human small-cell lung cancer (SCLC) lines CPH 54A and CPH 54B are subpopulations of the same patient tumor, and they have identical light microscopical morphology when grown as xenografts in immune deficient mice. In spite of their common genomic origin they represent considerably different phenotypes, as documented in previous studies. The 54A tumors are more radiosensitive than 54B *in vivo* [1], and *in vitro* [2]. The steady-state ATP levels are higher in 54A than in 54B when grown as solid tumors [3] and *in vitro*, correspondingly, the cellular ATP concentration in 54A cells is higher than in 54B cells [4]. The 54B tumors produce more lactate than 54A tumors, whereas the 54A tumors have a greater capacity for oxygen consumption [5]. Significant differences between the two tumor sublines in uptake and disposition kinetics of low-molecular-weight agents have been documented by ^{19}F magnetic resonance spectroscopy [6], ultrafast functional computed tomography [7], and by *ex vivo* whole tumor perfusion [5]. This intrinsic difference between the sublines 54A and 54B appears to outweigh the physiological impact of different transplantation modes [7,8]. Taken together these findings suggest that the two tumor lines represent different metabolic phenotypes with a glycolytic predominance of 54B. The underlying mechanism has not been clear. Quantitative differences in glucose uptake capacity could be one explanation of the dissimilarities between 54A and 54B. The present study was initiated with the aim of testing for such a difference, which we were able to document. Further we examined the expression of glucose transporters (GLUTs), the angiogenic vascular endothelial growth factor (VEGF), and their common transcriptional regulator hypoxia-inducible factor (HIF)-1α. Improved knowledge of the complex correlations between 2-fluoro-2-deoxy-D-glucose (FDG) uptake, GLUTs and angiogenesis provides important background information for further understanding of the glycolytic phenotype of solid tumors. Such information is pivotal for refined interpretation of clinical ^{18}FFDG positron emission tomography (PET) findings and for the development of therapies attacking metabolic and/or angiogenic regulators [9].

Materials and Methods

Cell Cultures

The human SCLC lines CPH 54A and 54B were maintained with modified Eagle's medium (MEM) with

Abbreviations: FDG, 2-fluoro-2-deoxy-D-glucose; GLUT-1, glucose transporter-1; HIF-1α, hypoxia inducible factor; PET, positron emission tomography; ROI, region of interest; SCLC, small-cell lung cancer; VEGF, vascular endothelial growth factor

Address all correspondence to: Dr. Paul E. G. Kristjansen, MD, PhD, Laboratory of Experimental Oncology, Molecular Pathology, University of Copenhagen, 11 Frederik V Vej, DK-2100 Copenhagen, Denmark. E-mail: paulk@pai.ku.dk

[1]Supported by the Danish Cancer Society (grant # 9810034 and grant # 99142069132) and by the Danish Medical Research Council (grant # 9702250).

Earle's salts containing GLUTAMAX-1 (L-alanyl-L-glutamine) (Gibco BRL) supplemented with 10% heat-inactivated FCS. The cells were cultured without addition of antibiotics in a humidified atmosphere with 5% CO_2 at 37°C.

Hypoxic Conditions In Vitro

Hypoxic conditions were established using BBL GasPak Anaerobic System (Becton Dickinson) according to the manufacturers directions.

Animals

Institutional guidelines for animal welfare and experimental conduct were followed. The mice were 8-week male nudes (NMRI *nu/nu*, M&B, Ry, Denmark). They were kept under sterile conditions in laminar airflow benches. The room temperature was 25±2°C, and the relative humidity was 55±5%. Sterile food and water was given *ad libitum*.

Tumor Xenografts

The SCLC tumor lines, CPH 54A and 54B, were maintained as serially transplanted xenografts *in vivo* in nude mice.

Mice were anaesthetized by subcutaneous (s.c.) injections of ketamine (10 mg/kg) and xylazine (1 mg/kg) in an isotonic 0.9% NaCl solution. Through a 1-cm incision in the dorsal skin, 1-mm^3 tumor blocks were subcutaneously implanted into both flanks. As a rule, 54A was inserted in the right flank and 54B in the left flank of the same mouse.

All treatments were carried out when tumors had reached a volume of approximately 500- to 600-mm^3, which generally occurred 2 to 3 weeks after transplantation.

FDG Uptake In Vivo

Tumor metabolic activity was estimated by measuring the FDG uptake *in vivo*. The tumor uptake of FDG was examined by PET, by use of an Advance GE scanner (General Electric Medical Systems, Milwaukee, WI) of nude mice carrying both 54A and 54B transplants, and by subsequent gamma counting of excised tumors.

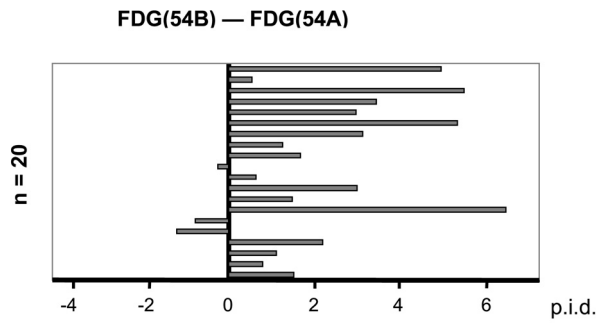

Figure 1. *In 20 mice a 54A tumor was grown at one flank and a 54B tumor at the other. The graph illustrates the distribution of differences in ^{18}F-FDG uptake (54B minus 54A) in each individual pair of one 54B tumor and one 54A tumor in the same mouse. This difference was negative in only 3 of 20 pairs, documenting that the uptake was greatest in 54B tumors ($P<.001$, Extreme range test for paired differences, Lords test). The uptake was calculated as percent of injected dose per volume (p.i.d.). 54A median p.i.d.: 4.94%, range: (2.62% to 8.84%); 54B median p.i.d.: 7.12%, range: 2.64% to 13.7%.*

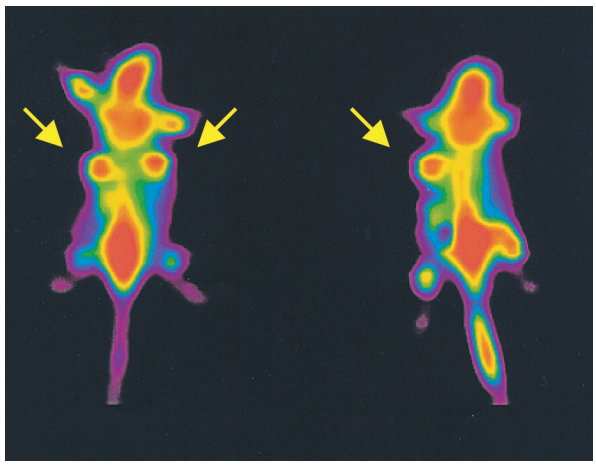

Figure 2. *PET scan of two tumor-bearing mice (Advance GE scanner, WI) following injection of 5 to 10 MBq of ^{18}F FDG. Arrows indicate tumor locations. In the animal at the right side a deposit was accidentally left at the injection side.*

[^{18}F]FDG was synthesized by the radiochemistry laboratory at the PET and cyclotron unit at the National University Hospital of Copenhagen, Denmark by nucleophilic substitution on mannose triphlate (1,3,4,6-tetra-*O*-acetyl-2-*O*-trifluoro-methanesulfonyl-β-D-mannopyranose) in automated systems.

For simultaneous PET scanning of six mice (12 tumors), a six-mice rack prototype was made of polyethylene. A dose of 5 to 10 MBq of FDG in 100 μl saline solution was injected into the tail veins. Using static PET scanning the FDG uptake was measured over 15 minutes. Before the emission scan, a transmission scan was performed for 10 minutes. PET images with an average slice thickness of 4.2 mm were generated by use of the filtered back projection reconstruction program. The maximal spatial resolution was 4 mm, and the image matrix was 256×256, whereas the pixel size in all reconstructed images was 1×1 mm^2. The images were corrected for attenuation and scatter. Regions of interest (ROIs) were defined as tumor volumes, and by PET the FDG uptake in 54A and 54B tumors were quantified by comparison of count rates for ROIs of the paired tumors in each animal.

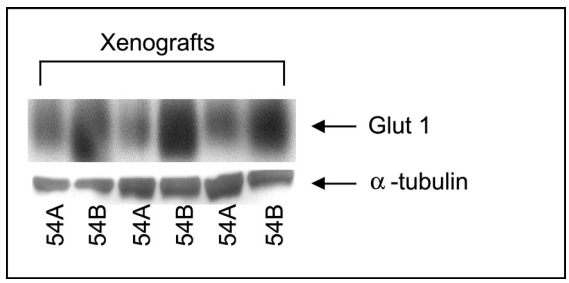

Figure 3. *Western blot of Glut-1 protein expression in 54A and 54B tumor xenografts. A higher Glut-1 expression in 54B tumors compared to 54A tumors. Lanes 1 and 2 were from the same animal as were 3 and 4, and 5 and 6. The quantitative, densitometric, ratios of Glut-1 to tubulin were significantly greater in 54B ($P<.05$), analysed with the extreme range test for paired differences, i.e., Lords test.*

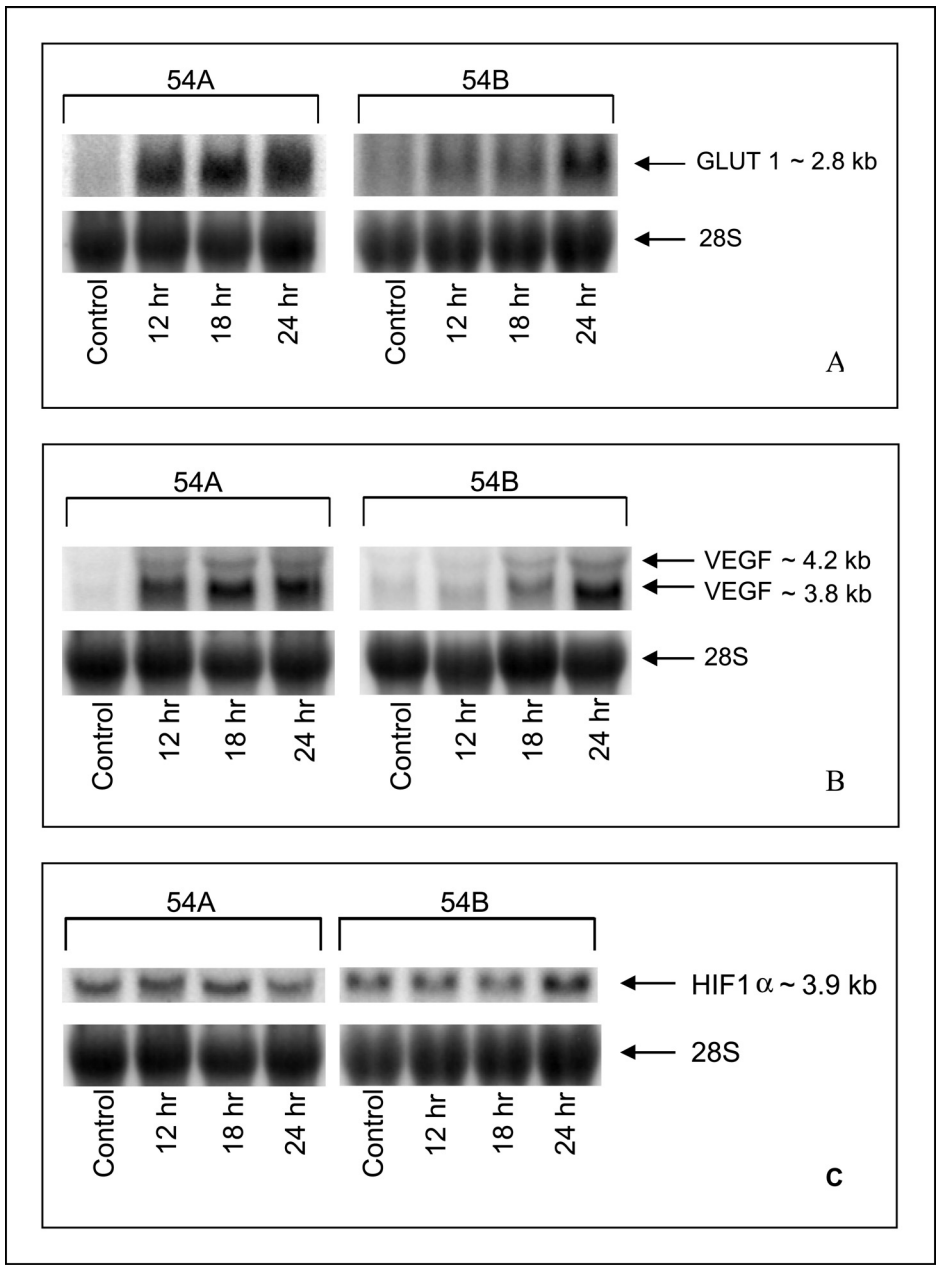

Figure 4. *Northern blots of GLUT-1 (A), VEGF (B), and HIF-1α (C) mRNA expression in 54A and 54B cell cultures grown under hypoxic conditions for 12, 18, and 24 hours, compared with normoxic controls. The loading control is 28S ribosomal RNA.*

Following the scanning procedure the tumors were excised, weighed, and gamma counted (Cobra 5003 Packard). The FDG uptake in the tumors was calculated as the specific biodistribution = (tumor activity/injected activity/gram of tumor weight) × 100%, i.e., the percent of injected dose per gram tumor tissue.

Hypoxic Conditions In Vivo

Tumor-bearing mice were transferred to an airtight chamber (kindly made available by Dr. Michael R. Horsman, Department of Experimental Clinical Oncology, Aarhus University Hospital, Denmark) and gassed with 10% oxygen for variable time periods. From previous studies of tumor-bearing mice we expected the oxygen partial pressure (pO_2) in the tumors to be severely reduced following 12 to 24 hours of exposure to 10% oxygen [10]. This protocol was applied because we wanted a sufficient degree of hypoxia, which, however, was not fatal to the mice, yet with a previously documented effect on hypoxia-sensitive gene expression. In the present series of experiments the resulting tumor pO_2 was not measured, because the tumors were excised and processed immediately when the chamber was opened. Three tumors of each type were examined for each of the time points.

Total RNA Isolation and Northern Blot Analysis

Total RNA was isolated with TRIZOL reagent (Life Technologies) following the directions of the manufacturer. Fifteen micrograms of total RNA of each sample was

subjected to electrophoresis on a 1% agarose gel containing 2% formaldehyde, stained with ethidium bromide, transferred to a GeneScreen Plus nylon membrane (NEN Research Products, DuPont), and hybridized to an [α-^{32}P]dCTP-labeled cDNA probe. Random priming was performed using the Rediprime DNA labelling kit (Amersham Pharmacia Biotech). Following labelling the membrane was washed in high-stringency conditions and exposed to a phosphoimager plate, and visualized on a STORM 840 phosphoimager (Molecular Dynamics).

The GLUT-1 and HIF-1α probes were polymerase chain reaction (PCR)-generated fragments with primers derived from the published cDNA sequences, whereas the 28S rRNA probe is commercially available (Clontech).

Primers for GLUT-1 were designed to amplify a 710-bp fragment (sense: 5′-TGGATGTCCTATCTGAGCATCG-3′, antisense: 5′-ATGGAACCATTCAGGGTGA AGC-3′). Primers for HIF-1α were designed to amplify a 622-bp fragment (sense: 5′-GAGGCTTACCATCAGCTATTTGCG-3′, antisense: 5′-CTGGCTCATACTCCATCAA TTCGG-3′).

The cDNA probes (PCR products) were purified from primers by centrifugation through a Micro SpinTM S-400 HR Column (Amersham Pharmacia Biotech) and verified by sequencing (ABI PRISM 310 Genetic Analyzer, Perkin-Elmer).

The 28S probe was labelled using the 5′-end labeling kit (Amersham, RPN 1509) and used as an internal control to normalize for differences in the quantity of total RNA loaded in each lane [11].

Western Blot Analysis

Tissue homogenate or cell lysate was sonicated five times for a few seconds by ultrasound using a Vibra Cell 50 (Sonics and Materials). Protein concentrations were determined using the BCA protein assay reagent (Pierce). SDS-PAGE was performed with 20 μg of total protein on precast 8% acrylamide Tris-glycine gels (NOVEX). Samples were denatured at 60°C before loading. After electrophoresis, the proteins were blotted to polyvinylidene difluoride membranes (NOVEX) using a semidry blotting device (Trans-blot SD BIORAD). Membranes were blocked with 5% BSA–Tris buffered saline containing 2.5% milk followed by incubation with mouse monoclonal antibodies raised against the NH_2 terminus of the human Glut-1, -3, and -4 proteins (F-18, F-68, and F-27). The antibodies were kindly provided by Dr. Peer Jørgensen, Novo Nordisk, Denmark. After several washes in Tris-buffered saline containing 0.1% Tween-20 (TBS-T), the membranes were incubated with a dilution of a horseradish peroxidase conjugated secondary antibody (Code No. P0447, Dako, Denmark), and washed several times in TBS-T. Finally the protein expression was detected with ECL+ (Amersham).

Results

FDG Uptake In Vivo

Bilaterally transplanted mice (n=20) carrying a 54A tumor xenograft in the right flank and a 54B tumor xenograft in the left flank, were used to examine FDG uptake *in vivo* by PET and subsequent gamma counting on excision of the tumors. By comparing two tumors in the same animal the bias induced by interanimal biologic variations, as well as by variations in the IV injection, was avoided.

In 17 of 20 mice the FDG uptake in 54B tumors were higher than in 54A tumors (Figure 1). Using the extreme range test for paired differences, i.e., Lords test, on 20 pairs of 54A and 54B tumors, a significantly higher FDG uptake per gram tissue was found in 54B tumors compared with 54A tumors (P<.001). By PET the tumors were clearly visualized (Figure 2) but we could not obtain sufficient resolution to distinguish quantitatively to what degree the PET activity (i.e., the FDG uptake) was different between 54A and 54B tumors.

Glucose Transporter Proteins

The protein expression of GLUTs in 54A and 54B tumors was examined by Western blotting. Figure 3 shows a

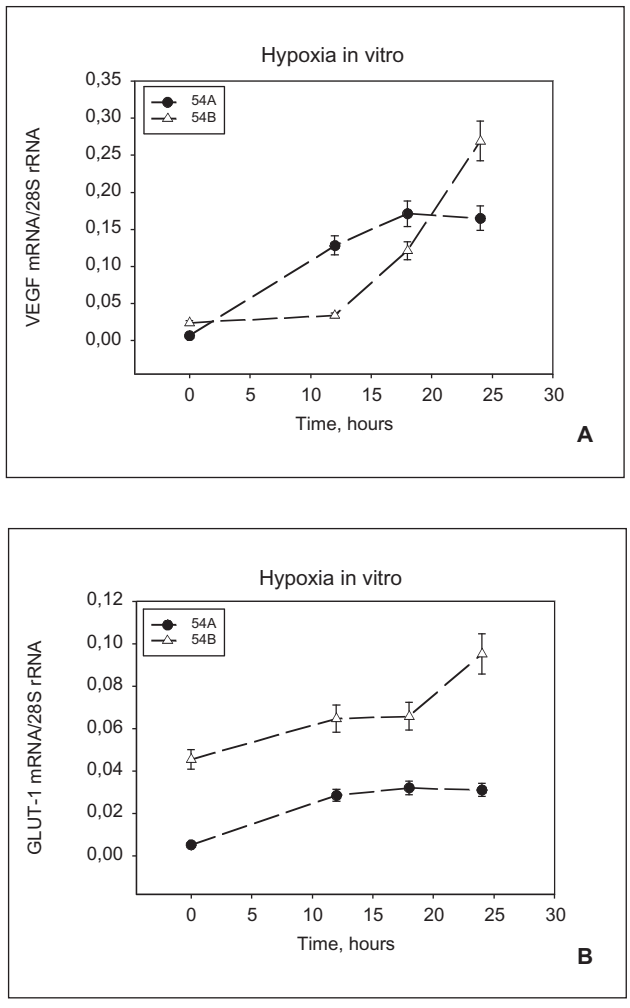

Figure 5. *VEGF and GLUT-1 mRNA in cell cultures. Relative expression of VEGF (A) and GLUT-1 (B) mRNA in 54A and 54B cells during hypoxia in vitro. A significant upregulation is seen in both cell lines. 54A levels off earlier than 54B. The GLUT-1 mRNA levels are constantly higher in 54B than in 54A. Each point represents cell cultures of between 5×10^6 and 9×10^6 cells. Bars represent standard error.*

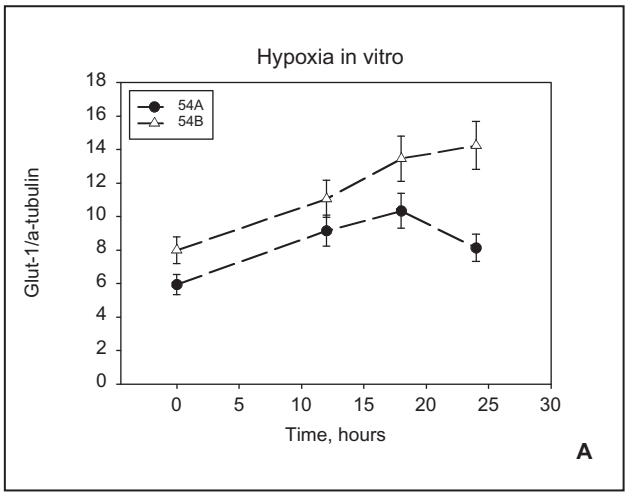

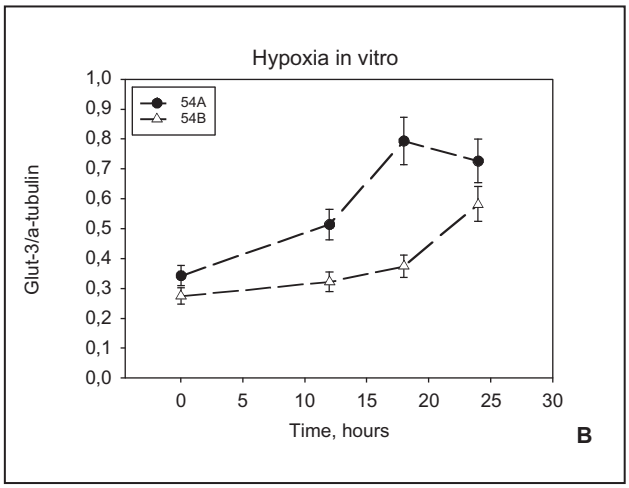

Figure 6. *Glut-1 and Glut-3 protein expression in cell cultures. Relative expression of Glut-1 (A) and Glut-3 (B) protein in 54A and 54B cell cultures grown under hypoxic conditions for 12, 18, and 24 hours, compared with normoxic controls. 54A levels off earlier than 54B. Each point represent cell cultures of between 5×10^6 and 9×10^6 cells. Bars represent standard error.*

representative western blot of the Glut-1 expression. Three pairs of 54A and 54B tumor xenografts were examined. As seen in Figure 3, Glut-1 migrates as a broad band of 45 to 55 kDa, which is due to variable glycosylation of the molecule [12]. When normalized by the α-tubulin expression, a significantly higher Glut-1 expression was found in 54B tumors compared to 54A tumors ($P<.05$). The Glut-1 levels determined by densitometry were 32%, 39%, and 67% greater in the 54B tumor in the three tumor pairs, respectively. No difference was found between the two lines with regard to the expression of Glut-3 and Glut-4 (data not shown).

Challenge with Hypoxia In Vitro

GLUT-1 and VEGF mRNA Figure 4*A* shows representative Northern blots of GLUT-1 mRNA and 28S rRNA expression following variable periods of exposure to hypoxia *in vitro*. The GLUT-1 mRNA corresponds to the band of 2.8 kb [13,14].

The mRNA hybridization signals on the Northern blots were quantified using densitometric scanning. The expression of 28S ribosomal RNA was used to normalize for differences in the quantity of total RNA loaded in each lane, and the ratio of GLUT-1 mRNA to 28S rRNA was calculated. Similarly a severalfold increase in VEGF mRNA, compared with the levels of mRNA present at normoxic conditions, was seen during hypoxia in 54A and 54B (Figure 4*B*). In Figure 5*A* and *B* quantitations of the GLUT-1 and the VEGF gene specific signals in arbitrary densitometric units are shown.

Glucose transporter proteins Western blots were performed to examine if there was any detectable regulation of Glut-1 and Glut-3 proteins following hypoxia. To correct for the slight variations in gel loading, the protein expression was normalized to the α-tubulin expression. The relative intensity was quantitated by densitometry. Both Glut-1 and Glut-3 proteins were upregulated by hypoxia *in vitro* in both cell lines (Figure 6, *A* and *B*).

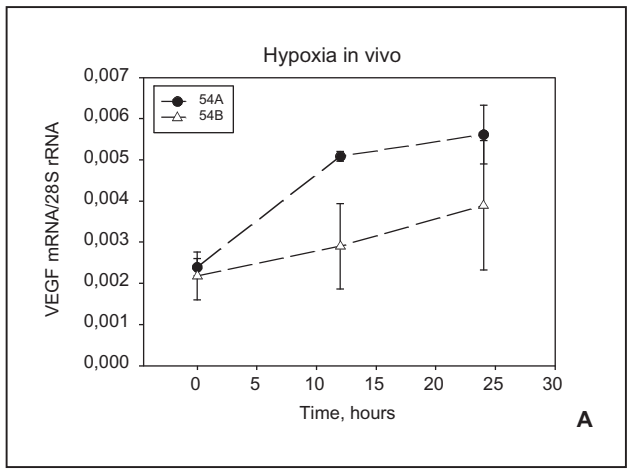

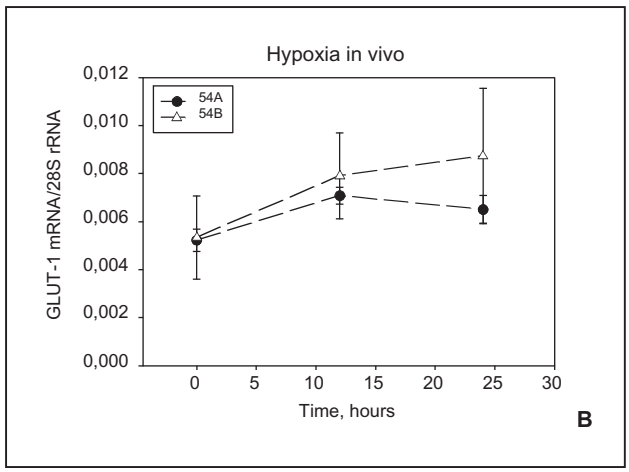

Figure 7. *VEGF and GLUT-1 mRNA from solid tumors. Relative expression of VEGF (A) and GLUT-1 (B) mRNA in 54A and 54B tumors during hypoxic incubation for 12 and 24 hours, compared with normoxic controls. Three tumors were examined for each of the time points. Bars indicate standard deviations.*

HIF-1α mRNA Figure 4*C* illustrates the HIF-1α mRNA expression in 54A and 54B following exposure to hypoxia. The HIF-1α mRNA expression corresponds to the band of 3.9 kb [15]. When normalized by the 28S rRNA expression there was no detectable change in HIF-1α mRNA following exposure to hypoxia.

Challenge with Hypoxia In Vivo

Figure 7*A* and *B* shows GLUT-1 and VEGF mRNA regulation in 54A and 54B following hypoxia *in vivo*. For both genes the mRNA upregulation in 54A did not increase beyond the 12-hour time point.

Discussion

The observed differences between the tumor subpopulations 54A and 54B in FDG uptake and Glut-1 expression adds substantially to the bulk of evidence [3–5] of a glycolytic predominance in 54B tumors relative to 54A. The tumor diameter of 10 mm and a spatial resolution of 4 mm did not permit us to obtain reliable quantitative data from the PET scans alone, but gamma counting of the excised tumors effectively documented a significantly different uptake. Future PET investigations of mice should probably apply the OSEM (ordered subset expectation maximization) reconstruction and attenuation correction [16].

The GLUT-1 and GLUT-3 genes are found transcriptionally upregulated in a variety of cancerous tissues compared with normal tissues. This phenomenon has been proposed as an explanation of the increased tumor uptake of glucose [13,14,17–19]. Concordantly, the greater FDG uptake in 54B tumors is likely to be a result of the correspondingly higher content of Glut-1 protein in this tumor line. Yet it is still unresolved whether the limiting process for glucose utilization and FDG uptake is transport or phosphorylation. In some instances, there appears to be a correlation between the expressed level of Glut-1 and FDG uptake [20–23]. In principle, however, higher levels of glucose transporter protein do not guarantee increased FDG accumulation by cancer cells. In other studies, metabolic trapping through phosphorylation of FDG appears more likely as the rate-limiting step in FDG accumulation [24].

The occurrence of low-oxygen conditions within tumors is a frequent phenomenon, which induces changes in cellular metabolism and gene regulation. The transcription factor HIF-1 has been identified as a critical component of the oxygen-signaling pathway, activating the transcription of genes encoding GLUTs, glycolytic enzymes, and VEGF [25,26], among others. Although increases in HIF-1α mRNA upon hypoxia have been reported [15], most studies so far have not demonstrated substantial regulation at this level, indicating that the regulation of HIF-1 occurs by translational and/or posttranslational mechanisms [27,28]. The nuclear subunit HIF-1β is a constitutively expressed nuclear protein, and the level of the α subunit is most likely to govern the activity of the HIF-1 complex. In the presence of molecular oxygen, at normoxia, HIF-1α is subject to continuous ubiquitination and proteasomal degradation [29,30]. Under hypoxic conditions, the ubiquitination of HIF-1α is reduced and this subunit translocates to the nucleus to join with HIF-1β [31], and subsequently bind to the hypoxia reactive elements at specific promoter regions.

VEGF and GLUT-1 mRNA were upregulated in both cell lines following challenge with hypoxia *in vitro*, but a different expression pattern was consistently observed in 54A and 54B. In each case the increased expression levelled off earlier in 54A than in 54B, suggesting that in 54A the acute response to hypoxia is faster but more short-lived. Previously, 54A tumors were found to have a greater capacity for O_2 consumption [5]. In the present study, it appeared that hypoxia induced a relatively greater increase in 54A than in 54B, which further adds to the conception that 54A is more sensitive to oxygen depletion than 54B.

Challenge with hypoxia also upregulated the expression of VEGF and GLUT-1 mRNA in solid tumors *in vivo*. The relative increase in VEGF mRNA steady-state level was higher *in vitro* as opposed to *in vivo*, possibly reflecting the degree of hypoxia (i.e., anoxia *in vitro* compared to hypoxia *in vivo)*. Furthermore, the higher increase in VEGF mRNA levels *in vitro* might be a result of the complex interactions of angiogenic stimulators and inhibitors in the *in vivo* environment.

The observed hypoxia-induced rise in the steady-state levels of the VEGF mRNA can occur partly due to increased transcription through HIF-1 [32], but also due to posttranscriptional mechanisms, including an increase in mRNA stability [33,34].

Similar to VEGF, the hypoxic induction of GLUT-1 can be mediated by transcriptional activation through HIF-1 as well as by posttranscriptional mRNA stabilization mechanisms [34]. However, the transcription rate of the GLUT-1 gene is dually regulated by hypoxia: GLUT-1 gene transcription is enhanced in response to a reduction in oxygen concentration *per se*, acting through HIF-1 paralleled by a stimulation of GLUT-1 transcription secondary to the associated inhibition of oxidative phosphorylation during hypoxia [35,36]. Transcriptional activation of VEGF and GLUT-1 is presumably mediated not only by HIF-1–induced transcription but also by other transcription factors.

In the present series of experiments we found upregulated levels of GLUT-1 mRNA as well as Glut-1 and Glut-3 protein in both cell lines following exposure to hypoxia. The increased levels of GLUT-1 mRNA is likely to be the result of increased transcription probably partly through HIF-1 and partly as a consequence of decreased oxidative phosphorylation.

The observed increase in cellular Glut-1 and Glut-3 proteins during hypoxia must have been caused by translational and/or posttranslational mechanisms. The rise in Glut-1 protein expression is likely to be a result of *de novo* synthesis of the transporter, because we found increased levels of GLUT-1 mRNA. To what degree the proteins are active is unknown. It is possible that some of the Glut-1 proteins are stored in intracellular vesicles or that some of the Glut-3 proteins remain inactive in the membrane. The just below two-fold increase in Glut-1 protein (Figure 6*A*)

did not match the six-fold increase found in GLUT-1 mRNA in 54A (Figure 5*A*), indicating that not all GLUT-1 mRNA is translated in 54A, or that the turnover of Glut-1 protein is increased.

In summary, a significantly higher FDG uptake was found in the SCLC subpopulation 54B compared to its syngeneic counterpart 54A. Correspondingly, a significantly higher expression of the glucose transporter Glut-1 was observed, whereas the expression of Glut-3 and Glut-4 was similar in the two SCLC sublines. The GLUT-1 expression was coregulated with VEGF in both lines both *in vivo* and *in vitro*, but a consistently different regulation pattern following hypoxic stress was observed in the two sister lines 54A and 54B.

The present data represent steps toward a further understanding of the crucial relationship between angiogenesis, glycolysis, and hypoxia. Further clarification of these correlations may even elucidate to what extent PET examination can detect microscopic angiogenic foci representing residual disease or relapse in cancer patients. The present set of data also constitutes a platform for testing of new therapeutic agents directed against the HIF-1 function.

Acknowledgements

We thank H.A. Weich, Braunschweig, Germany for providing VEGF cDNA.

References

[1] Spang-Thomsen M, Clerici M, Engelholm SA, and Vindelov LL (1986). Growth kinetics and *in vivo* radiosensitivity in nude mice of two subpopulations derived from a single human small cell carcinoma of the lung. *Eur J Cancer Clin Oncol* **22**, 549–556.

[2] Krarup M, Poulsen HS, and Spang-Thomsen M (1997). Cellular radiosensitivity of small-cell lung cancer cell lines. *Int J Radiat Oncol Biol Phys* **38**, 191–196.

[3] Kristjansen PEG, Pedersen EJ, Quistorff B, Elling F, and Spang-Thomsen M (1990). Early effects of radiotherapy in small cell lung cancer xenografts monitored by ^{31}P magnetic resonance spectroscopy and biochemical analysis. *Cancer Res* **50**, 4880–4884.

[4] Kristjansen PEG, Spang-Thomsen M, and Quistorff B (1991). Different energy metabolism in two human small cell lung cancer subpopulations examined by ^{31}P magnetic resonance spectroscopy and biochemical analysis *in vivo* and *in vitro*. *Cancer Res* **51**, 5160–5164.

[5] Kristjansen PEG, Brown TJ, Shipley LA, and Jain RK (1996). Intratumor pharmacokinetics, flow resistance, and metabolism during gemcitabine infusion in *ex vivo* perfused human small cell lung cancer. *Clin Cancer Res* **2**, 359–367.

[6] Kristjansen PEG, Quistorff B, Spang-Thomsen M, and Hansen HH (1993). Intratumoral pharmacokinetic analysis by 19-F magnetic resonance spectroscopy and cytostatic *in vivo* activity of Gemcitabine in two small cell lung cancer xenografts. *Ann Oncol* **4**, 157–160.

[7] Hamberg LM, Kristjansen PEG, Hunter GJ, Wolf GL, and Jain RJ (1994). Spatial heterogeneity in tumor perfusion measured with functional computed tomography at 0.05 μl resolution. *Cancer Res* **54**, 6032–6036.

[8] Kristjansen PEG (1997). Pathophysiology of human tumor xenografts. Aspects of metabolism, physiology, and pharmacokinetics in heterotransplanted human lung and colon tumors. *Dan Med Bull* **44** 380–395.

[9] Kung AL, Wang S, Klco JM, Kaelin WG, and Livingston DM (2000). Suppression of tumor growth disruption of hypoxia-inducible transcription. *Nat Med* **6**, 1335–1340.

[10] Ehrnrooth E, von der Maase H, Sorensen BS, Poulsen JH, and Horsman MR (1999). The ability of hypoxia to modify the gene expression of thymidylate synthase in tumour cells *in vivo*. *Int J Radiat Biol* **75**, 885–891.

[11] Zhong H, and Simons JW (1999). Direct comparison of GAPDH, beta-actin, cyclophilin, and 28S rRNA as internal standards for quantifying RNA levels under hypoxia. *Biochem Biophys Res Commun* **259** (3), 523–526.

[12] Koseoglu MH, and Beigi FI (1999). Mechanism of stimulation of glucose transport in response to inhibition of oxidative phosphorylation: analysis with myc-tagged Glut1. *Mol Cell Biochem* **194**, 109–116.

[13] Yamamoto T, Seino Y, Fukumoto H, Koh G, Yano H, Inagaki N, Yamada Y, Inoue K, Manabe T, and Imura H (1990). Over-expression of facilitative glucose transporter genes in human cancer. *Biochem Biophys Res Commun* **170**, 223–230.

[14] Au KK, Liong E, Li JY, Li PS, Liew CC, Kwok TT, Choy YM, Lee CY, and Fung KP (1997). Increases in mRNA levels of glucose transporters types 1 and 3 in Ehrlich ascites tumor cells during tumor development. *J Cell Biochem* **67**, 131–135.

[15] Wang GL, Jiang BH, Rue EA, and Semenza GL (1995). Hypoxia-inducible factor 1 is a basic-helix–loop–helix–PAS heterodimer regulated by cellular O2 tension. *Proc Natl Acad Sci USA* **92**, 5510–5514.

[16] Hudson HM, and Larkin RS (1994). Accelerated image reconstruction using ordered subsets of projection data. *IEEE Trans Med Imaging* **13**, 601–609.

[17] Binder C, Binder L, Marx D, Schauer A, and Hiddemann W (1997). Deregulated simultaneous expression of multiple glucose transporter isoforms in malignant cells and tissues. *Anticancer Res* **17**, 4299–4304.

[18] Younes M, Lechago LV, Somoano JR, Mosharaf M, and Lechago J (1996). Wide expression of the human erythrocyte glucose transporter Glut1 in human cancers. *Cancer Res* **56**, 1164–1167.

[19] Suzuki T, Iwazaki A, Katagiri H, Oka Y, Redpath JL, Stanbridge EJ, and Kitagawa T (1999). Enhanced expression of glucose transporter GLUT3 in tumorigenic HeLa cell hybrids associated with tumor suppressor dysfunction. *Eur J Biochem* **262**, 534–540.

[20] Higashi T, Tamaki N, Honda T, Torizuka T, Kimura T, Inokuma T, Ohshio G, Hosotani R, Imamura M, and Konishi J (1997). Expression of glucose transporters in human pancreatic tumors compared with increased FDG accumulation in PET study. *J Nucl Med* **38**, 1337–1344.

[21] Brown RS, Leung JY, Fisher SJ, Frey KA, Ethier SP, and Wahl RL (1996). Intratumoral distribution of tritiated-FDG in breast carcinoma: correlation between Glut-1 expression and FDG uptake. *J Nucl Med* **37**, 1042–1047.

[22] Chung JK, Lee YJ, Kim C, Choi SR, Kim M, Lee K, Jeong JM, Lee DS, Jang JJ, and Lee MC (1999). Mechanisms related to [F-18]fluorodeoxyglucose uptake of human colon cancers transplanted in nude mice. *J Nucl Med* **40**, 339–346.

[23] Waki A, Kato H, Yano R, Sadato N, Yokoyama A, Ishii Y, Yonekura Y, and Fujibayashi Y (1998). The importance of glucose transport activity as the rate-limiting step of 2-deoxyglucose uptake in tumor cells *in vitro*. *Nucl Med Biol* **25**, 593–597.

[24] Aloj L, Caraco C, Jagoda E, Eckelman WC, and Neumann RD (1999). Glut-1 and hexokinase expression: relationship with 2-fluoro-2-deoxy-D-glucose uptake in A431 and T47D cells in culture. *Cancer Res* **59**, 4709–4714.

[25] Wang GL, and Semenza GL (1993). Characterization of hypoxia-inducible factor 1 and regulation of DNA binding activity by hypoxia. *J Biol Chem* **268**, 21513–21518.

[26] Wang GL, and Semenza GL (1993). General involvement of hypoxia-inducible factor 1 in transcriptional response to hypoxia. *Proc Natl Acad Sci USA* **90**, 4304–4308.

[27] Huang LE, Arany Z, Livingston DM, and Bunn HF (1996). Activation of hypoxia-inducible transcription factor depends primarily upon redox-sensitive stabilization of its alpha subunit. *J Biol Chem* **271**, 32253–32259.

[28] Wenger RH, Kvietikova I, Rolfs A, Gassmann M, and Marti HH (1997). Hypoxia-inducible factor-1 alpha is regulated at the post-mRNA level. *Kidney Int* **51**, 560–563.

[29] Huang LE, Gu J, Schau M, and Bunn H (1998). Regulation of hypoxia-inducible factor 1α is mediated by an O_2-dependent degradation domain *via* the ubiquitin–proteasome pathway. *Proc Natl Acad Sci USA* **95**, 7987–7992.

[30] Kallio PJ, Wilson WJ, O'Brian S, Makino Y, and Poellinger L (1999). Regulation of the hypoxia-inducible transcription factor 1α by the ubiquitin–proteasome pathway. *J Biol Chem* **274**, 6519–6525.

[31] Sutter CH, Laughner E, and Semenza GL (2000). Hypoxia-inducible factor 1α protein expression is controlled by oxygen-regulated ubiquitination that is disrupted by deletions and missense mutations. *Proc Natl Acad Sci USA* **97**, 4748–4753.

[32] Forsythe JA, Jiang BH, Iyer NV, Agani F, Leung SW, Koos RD, and Semenza GL (1996). Activation of vascular endothelial growth factor gene transcription by hypoxia-inducible factor 1. *Mol Cell Biol* **16**, 4604–4613.

[33] Ikeda E, Achen MG, Breier G, and Risau W (1995). Hypoxia-induced transcriptional activation and increased mRNA stability of vascular endothelial growth factor in C6 glioma cells. *J Biol Chem* **270** 19761–19766.

[34] Stein I, Neeman M, Shweiki D, Itin A, and Keshet E (1995). Stabilization of vascular endothelial growth factor mRNA by hypoxia and hypoglycemia and coregulation with other ischemia-induced genes. *Mol Cell Biol* **15**, 5363–5368.

[35] Behrooz A, and Ismail BF (1997). Dual control of glut1 glucose transporter gene expression by hypoxia and by inhibition of oxidative phosphorylation. *J Biol Chem* **272**, 5555–5562.

[36] Shetty M, Ismail BN, Loeb JN, and Ismail BF (1993). Induction of GLUT1 mRNA in response to inhibition of oxidative phosphorylation. *Am J Physiol* **265**, C1224–C1229.